Alternative Model for the Internal Structure of Laminin†

Sally L. Palm, James B. McCarthy, and Leo T. Furcht*

Department of Laboratory Medicine and Pathology, The University of Minnesota, Minneapolis, Minnesota 55455

Received March 22, 1985

ABSTRACT: A monoclonal antibody to laminin, LMN-1, was generated by immunizing rats with laminin from the EHS tumor and fusing the rat spleen cells with mouse NS-1 myeloma cells. Laminin fragments were generated by proteolytic digestion with thrombin, thermolysin, and chymotrypsin. Monoclonal antibody binding fragments were identified by immunoblotting. Fragments which bound monoclonal antibody LMN-1 included a 440-kilodalton (kDa) chymotrypsin fragment and thermolysin fragments of 440 and 110 kDa. These fragments could also be generated from within a 600-kDa thrombin fragment. Digestion of the 440-kDa chymotrypsin fragment with thermolysin generated the 110-kDa antibody binding fragment and a 330-kDa nonbinding fragment. Immunoblotting was performed on extracts of PYS-2 cells and EHS cells using polyclonal and monoclonal antibodies to laminin. Polyclonal antibodies stained the intact 850-kDa complex and the 200- and 400-kDa subunits, while monoclonal LMN-1 stained only the 400-kDa subunit and the complete molecule. Rotary shadowing of monoclonal LMN-1 bound to laminin molecules indicated that the binding site was within the long arm of laminin. Changes in the model of the internal organization of the laminin molecule are proposed, based on the binding of LMN-1 to the 400-kDa subunit and specific proteolytic fragments. The locations of the major thrombin and chymotrypsin fragments in the model are rotated 180° relative to the previously described model [Ott, U., Odermatt, E., Engel, J., Furthmayr, H., & Timpl, R. (1982) *Eur. J. Biochem. 123*, 63–72] to include part of the 400-kDa subunit of laminin.

Laminin is a high molecular weight glycoprotein (M_r 850 000) found in basement membranes throughout the body and produced by a variety of cells in vivo and in vitro (Timpl et al., 1979; Foidart et al., 1982; Palm & Furcht, 1983). Large quantities of laminin can be isolated in an intact form from the murine EHS tumor, where it consists of subunits of 200 and 400 kilodaltons (kDa) that are thought to be disulfide bonded as a trimer of 200-kDa subunits with a single 400-kDa subunit (Engel et al., 1981). The laminin molecule appears cross-shaped by rotary shadowing, with one long arm and three short arms (Engel et al., 1981). As has been seen with other large protein molecules such as fibronectin, laminin can be involved in multiple types of interactions. These interactions include binding of laminin to proteins (i.e., type IV collagen; Terranova et al., 1983) and glycosaminoglycans (Sakashita et al., 1980; Del Rosso et al., 1981), mediating the adhesion of cells to substrates (Terranova et al., 1980; Palm & Furcht, 1983; Vlodavsky & Gospodarowicz, 1981; Couchman et al., 1983) and other cells (Ozawa et al., 1983) and promoting motility of cells (McCarthy et al., 1983; McCarthy & Furcht, 1984). Studies on proteolytic fragments of laminin indicate that these interactions may be mediated by specific functional domains or regions within the laminin molecule. For example, Rao et al. (1982b) used thrombin to produce a 600-kDa fragment of laminin which mediated the attachment of human squamous carcinoma cells to type IV collagen. Pepsin and cathepsin G have been used to produce a fragment of laminin, called P1, which binds to a cell-surface laminin receptor but does not interact with type IV collagen (Terranova et al., 1983).

Assigning functional domains to actual physical locations within a molecule requires "landmarks" on the molecule for identification and placement of fragments. The laminin fragments localized thus far have been placed by comparing rotary shadowing images of fragments with images of the intact molecule. This is a purely visual technique, making it difficult to unambiguously localize fragments. Another method of localization uses monoclonal antibodies as the landmarks on the molecules. This allows immunological identification and localization of fragments by such techniques as immunoprecipitation, immunoblotting, and enzyme immunoassays, as well as visual localization by rotary shadowing on antibody–antigen complexes. In this paper, we describe the production and characterization of a monoclonal antibody against laminin, the reaction of the monoclonal antibody with proteolytic fragments of laminin, several of which have known functions, and the use of the monoclonal antibody in redefining the internal structure of the laminin molecule.

Materials and Methods

Reagents. Reagents were purchased from the following companies: Dulbecco's modified Eagle's medium (DMEM) and 100× antibiotic/antimycotic solution, Grand Island Biologicals, Grand Island, NY; heat-inactivated horse serum, Sterile Systems, Inc., Logan, UT; fetal bovine serum, Grand Island Biologicals, Grand Island, NY, or Hazelton-Dutchland, Inc., Denver, PA; peroxidase-conjugated goat anti-rat and goat anti-rabbit immunoglobulin G (IgG) and rabbit anti-rat IgG, Cooper Biomedical/Cappel Laboratories, Malvern, PA; acrylamide, thermolysin, and dithiothreitol, Sigma Chemical Co., St. Louis, MO; bis(acrylamide) and sodium dodecyl sulfate (SDS), Bio-Rad Laboratories, Richmond, CA; chymotrypsin, Worthington Biochemical Co., Freehold, NJ; immobilized soybean trypsin inhibitor and immobilized *p*-chlorobenzamide, Pierce Chemical Co., Rockford, IL; nitrocellulose paper type HAHY, Millipore Corp., Bedford, MA;

†This research was supported by National Cancer Institute, National Institutes of Health (NCI/NIH), Grants CA29995 and CA21463 and a grant from the Leukemia Task Force. L.T.F. is a recipient of a Stone Professorship of Pathology, The University of Minnesota, and Research Career Development Award CA00651 from NCI/NIH. J.B.M. is supported by NCI/NIH Grant CA39510.

0006-2960/85/0424-7753$01.50/0

En^{3}Hance autoradiography enhancer, New England Nuclear, Boston, MA; [^{35}S]methionine, Amersham, Arlington Heights, IL; Kodak XAR5 autoradiography film, Eastman Kodak, Rochester, NY; *Staphylococcus aureus* V8 protease, Miles Laboratories, Elkhart, IN; dispase (neutral protease), Boehringer-Mannheim Biochemicals, Indianapolis, IN. Thrombin was a gift from Dr. John Fenton, New York State Department of Health, Albany, NY. Lewis rats, 125–150 g, were purchased from Harlan Sprague Dawley, Madison, WI.

Protein Purification. Laminin was isolated from the EHS tumor by using methods described previously (Palm & Furcht, 1983).

Cell Culture. PYS-2 mouse parietal yolk sac carcinoma cells were originally a gift from Dr. Davor Solter, Wistar Institute, Philadelphia, PA. Cells were maintained in DMEM containing 10% heat-inactivated horse serum. EHS tumor cells were isolated for primary cultures by pressing tumor tissue through a mesh screen and digesting cells from the matrix for 2–4 h with dispase and collagenase in Dulbecco's phosphate-buffered saline (PBS; 1 mg/mL sample of each enzyme). Cells were washed twice with DMEM containing 10% fetal bovine serum, plated on 100-mm tissue culture plates in the same medium with antibiotic/antimycotic reagents (100 units/mL penicillin, 100 μg/mL streptomycin, and 20 μg/mL fungizone), and fed with this medium every 4 days. (Note: EHS cells do not appear to proliferate but are able to survive for 1–2 weeks under these culture conditions.)

Immunoprecipitation. Cells were labeled for 2 h with 200 μCi/mL [^{35}S]methionine or overnight with 50 μCi/mL methionine in serum-free DMEM. Immunoprecipitation and dissociation of precipitates under reducing conditions were performed as previously described (Palm & Furcht, 1983). The immunoprecipitation samples were separated on 2–15% gradient SDS–polyacrylamide gels, stained with Coomassie Blue R250, treated with En^{3}Hance, and dried. Fluorography was performed with Kodak XAR5 film.

Monoclonal Antibody Production. Male Lewis rats were immunized by subcutaneous injection with 50–100 μg of laminin in complete Freund's adjuvant, followed by two to four subcutaneous booster injections of laminin in incomplete Freund's adjuvant. Rats were given a final tail vein injection of 25–50 μg of laminin in saline 3 days prior to harvesting spleen cells for fusion. Isolated spleen cells were fused with P3-NS1-AG4-1 mouse myeloma cells (NS-1 cells) and grown as previously described (Smith & Furcht, 1982). Fused cells were screened for antibody production by the enzyme-linked immunosorbent assay (ELISA). Antibody-producing cells were cloned by limiting dilution using 96-well plates containing (2.0–3.0) × 10^4 NS-1 cells per well to serve as a "feeder" population. The NS-1 cells were plated 24 h prior to cloning in 100 μL/well of DMEM with 20% horse serum. At cloning, the antibody-producing cells were diluted in DMEM with 20% horse serum containing 24 mM hypoxanthine, 18 μM aminopterin, and 16 mM thymidine (2× HAT), and 100 μL of cell suspension was added per well, giving a final HAT concentration sufficient to kill the NS-1 feeder cells over a period of 1 week. Clones were screened periodically for antibody production by ELISA.

Antibody was produced by growing cloned hybrid cells in spinner flasks in HAT medium. Conditioned medium was collected at the time of subculturing and frozen until 500–1000 mL could be pooled. Antibody was isolated from conditioned medium by ammonium sulfate precipitation (50% of saturation). Precipitated antibody was dialyzed against PBS, titered by ELISA, and stored in aliquots at −70 °C.

Enzyme Digestions. Laminin in PBS with 0.75 mM $CaCl_2$ was digested at 37 °C with thermolysin or chymotrypsin at a 1:50 enzyme to protein ratio or at 22 °C with thrombin at a 1:70 enzyme to protein ratio. Digests were stopped by adding 0.1 volume of the following inhibitors: 0.2 M ethylenediaminetetraacetic acid (EDTA) for thermolysin; agarose-bound soybean trypsin inhibitor for chymotrypsin; agarose-bound *p*-chlorobenzamide for thrombin.

Electrophoresis and Peptide Mapping. Samples were separated on 2–15% sodium dodecyl sulfate (SDS)–polyacrylamide gradient gels with 2% stacking gels. Gel formulations were based on those of Blattler et al. (1972) using the buffer system of Laemmli (1970). Nonreducing electrophoresis sample buffer consisted of 0.08 M tris(hydroxymethyl)aminomethane (Tris), pH 6.8, 3% (w/v) SDS, 15% (v/v) glycerol, and 0.01% bromophenol blue. Nonreduced/reduced peptide maps of fragments were produced by separating samples under nonreducing conditions on gels, which were stained with Coomassie Brilliant Blue G-250 and destained in 7.5% methanol/7.5% acetic acid. Bands of interest were cut from the gel, incubated in three changes (15 min each) of equilibration buffer [62.4 mM Tris, pH 6.8, 2.3% (w/v) SDS, 10% (w/v) glycerol, 0.01% bromophenol blue, and 10 mg/mL dithiothreitol], and placed into the wells of a 2% stacking gel on a 2–15% gradient gel for the second electrophoresis run. Proteolytic peptide maps of the 400- and 200-kDa subunits of intact laminin and the 200-kDa band of the thrombin fragment were prepared following the method of Cleveland et al. (1977), the only modification being increasing the *Staphylococcus aureus* V8 protease digestion time from 30 to 60 min. The protein molecular weight markers used for gels included the following: human plasma fibronectin (nonreduced), 440 000; human plasma fibronectin (reduced), 220 000; phosphorylase *a*, 94 000; bovine serum albumin, 68 000; ovalbumin, 43 000; soybean trypsin inhibitor, 21 000; cytochrome *c*, 12 500. Final gels were stained with Coomassie Blue R-250.

Immunoblots. Protein fragments were separated on SDS–polyacrylamide gels in triplicate. Duplicate gels were transferred to nitrocellulose paper following the method for proteins in SDS described by Towbin et al. (1979). One blot was stained for protein by using amido black (0.02% in 45% methanol and 10% acetic acid) and the other blot prepared for immunostaining by soaking in 1% (w/v) bovine serum albumin (BSA) in PBS for a minimum of 1 h. The third nontransferred gel was stained with Coomassie blue and dried. Blots were immunostained by incubating in a 1:50 dilution of monoclonal antibody LMN-1 in 1% BSA/PBS with 10% (v/v) goat serum (30 min), washed in two changes of PBS (15 min each), incubated with a 1:500 dilution of peroxidase-conjugated goat anti-rat IgG in 1% BSA/10% goat serum PBS (30 min), washed with PBS (2 × 15 min), and reacted with 0.01% 3,3′-diaminobenzidine/0.003% hydrogen peroxide in PBS. The enzymatic reaction was stopped by rinsing the blot with large volumes of deionized water.

Extraction of Laminin from Cell Cultures. PYS-2 cells were grown to confluence in 100-mm tissue culture plates. EHS primary cell cultures were used as originally plated in the 100-mm plates. Cells were washed 3 times with PBS containing 0.75 mM $CaCl_2$. Cells from two plates were solubilized into 1 mL of nonreducing electrophoresis sample buffer (described above) and immediately electrophoresed on 2–15% gradient SDS–polyacrylamide gels. Immunoblots were prepared as described above. Because of problems of viscosity due to the DNA, samples in later studies were solubilized into

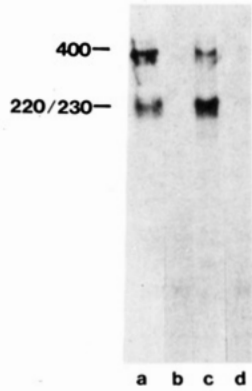

FIGURE 1: Immunoprecipitation of laminin from PYS-2 cell cultures metabolically labeled with [^{35}S]methionine. Lane a, monoclonal antibody; lane b, control supernatant from nonproducing hybridoma culture; lane c, affinity-purified polyclonal rabbit anti-laminin antibody; lane d, preimmune rabbit serum.

immunoprecipitation solubilization buffer (Palm & Furcht, 1983), mixed 1:1 with nonreducing electrophoresis sample buffer, and separated on gels as described above. Results using the two methods were similar.

Rotary Shadowing. Monoclonal antibody LMN-1 used for rotary shadowing was affinity-purified on a laminin–agarose column using 0.2 M glycine, pH 2.3, for elution of bound antibody. The antibody was dialyzed against PBS and stored at −70 °C until use. Antibody was mixed with purified laminin to give final concentrations of 40 μg/mL antibody and 80 μg/mL antigen. The mixture was dialyzed against 0.2 M ammonium bicarbonate, mixed with glycerol (to 60% v/v), and sprayed on freshly cleaned mica according to the methods of Kuhn et al. (1981) and Sauk et al. (1984). Rotary shadowing was performed in a modified Balzers freeze–fracture unit using carbon/platinum (95%:5%) at an angle of 6°. Specimens were stabilized by coating with carbon at an angle of 90°. Specimens were viewed with a Philips EM300 transmission electron microscope at 60 kV.

RESULTS

Characterization of Monoclonal Antibody. A monoclonal antibody against EHS laminin, LMN-1, was characterized by ELISA, immunoblotting, and immunoprecipitation. By ELISA, the antibody preparation reacted with laminin to a dilution of 1:80 but did not react with fibronectin or type IV collagen (other constituents of basement membrane) at any concentration. The antibody reacted with intact laminin, but not reduced or reduced and alkylated laminin, on immunoblots (blot not shown). LMN-1 antibody was used to precipitate metabolically radiolabeled laminin from cultures of PYS-2 cells. The monoclonal antibody precipitated protein, which under reducing conditions appeared as bands at 220/230 and at 400 kDa (Figure 1, lane a). These bands were identical with those precipitated by affinity-purified polyclonal rabbit anti-laminin antibodies (Figure 1, lane c) and matched the description of laminin from PYS-2 cultures given by other laboratories (Cooper et al., 1981; Howe & Dietzschold, 1983; Leivo, 1983). Lanes b and d are supernatants from a nonproducing hybridoma and preimmune rabbit serum controls, respectively.

Localization of Antibody Binding Regions in EHS Laminin. The region of the EHS laminin molecule recognized by monoclonal antibody LMN-1 was localized by proteolytically degrading laminin with thrombin, chymotrypsin, and/or thermolysin and performing immunoblots. Laminin was degraded with enzymes for 0.5–24 h. Because laminin contains

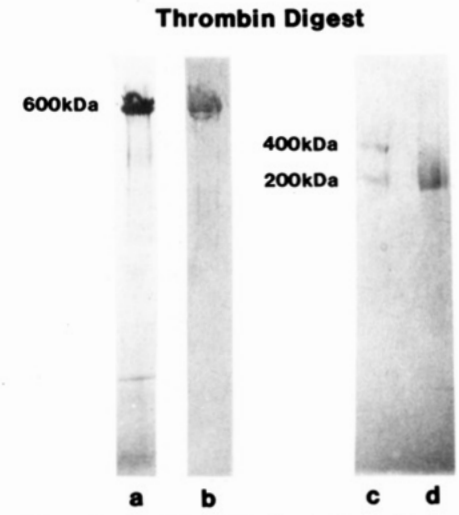

FIGURE 2: Monoclonal antibody binding to thrombin fragments of laminin. Lane a, 24-h thrombin digest, nonreduced. Coomassie blue stained SDS–polyacrylamide gel, 2–15% gradient. Lane b, gel transfer immunolocalization of monoclonal antibody binding to fragments generated by 24-h thrombin digestion. Lane c, reduced intact laminin. Coomassie blue stained SDS–polyacrylamide gel, 2–15% gradient. The two bands are the 200- and 400-kDa subunits of laminin reduced by treatment with 10 mg/mL dithiothreitol. Lane d, reduced 24-h thrombin digest of laminin. The large thrombin fragment reduces to a band at 200 kDa. The 400-kDa subunit of laminin has been digested by thrombin.

regions that are fairly resistant to proteolysis, only the later time points (7 and 24 h), when smaller fragments were generated, will be discussed.

Monoclonal antibody LMN-1 was first reacted with thrombin fragments of laminin. A nonreduced gel of a 24-h thrombin digest is shown in Figure 2, lane a. The prominent band is a 600-kDa thrombin fragment which has previously been described by Rao et al. (1982a). This fragment was recognized by the LMN-1 antibody on immunoblots (Figure 2, lane b). To verify that complete digestion had occurred, the thrombin digest was reduced with 10 mg/mL dithiothreitol and subjected to electrophoresis, along with a sample of intact laminin reduced in the same manner. The SDS gel of the reduced proteins shows the 200- and 400-kDa subunits of intact laminin (Figure 2, lane c) and the 200-kDa band of the reduced thrombin fragment (Figure 2, lane d). The 400-kDa subunit of laminin was digested by the thrombin.

Chymotrypsin and thermolysin were also used to generate laminin fragments. The fragments generated by 24-h chymotrypsin digestion are shown in Figure 3, lane a. The major fragment produced is 440 kDa in size (it comigrates with nonreduced plasma fibronectin at 440 kDa on gels), with other fragments being 50 kDa and below. Only the 440-kDa fragment reacted with LMN-1 on immunoblots (Figure 3, lane b). Seven-hour thermolysin digestion generated 10 distinct bands seen on nonreducing gels (Figure 3, lane c), including two large fragments at 440 and 330 kDa, a diffuse band at 110 kDa, and smaller bands from 30 to 80 kDa. With 24 h of thermolysin digestion, the 440-kDa fragment disappears, and the 330- and 110-kDa bands become more diffuse (Figure 3, lane d). LMN-1 antibody reacts with the largest (440 kDa) thermolysin fragment, and also the 110-kDa fragment, but not the 330-kDa or any smaller fragments in the 7-h digest (Figure 3, lane e). In the 24-h digest, the monoclonal antibody reacts only with the 110-kDa fragment (Figure 3, lane f).

Immunoblot studies on chymotrypsin and thermolysin digests of the 600-kDa thrombin fragment were performed next to determine whether the 440- and 110-kDa LMN-1 binding

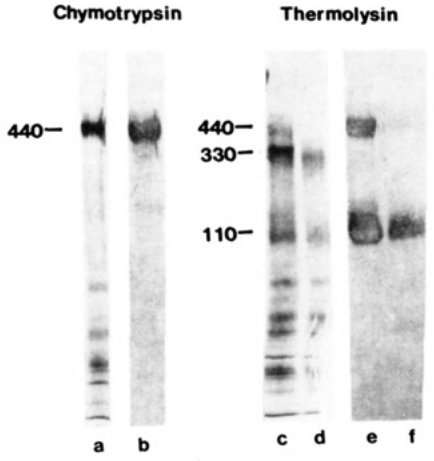

FIGURE 3: Monoclonal antibody binding to chymotrypsin and thermolysin fragments of laminin derived from the EHS tumor. Lane a, 24-h chymotrypsin digest. Coomassie blue stained SDS–polyacrylamide gel, 2–15% gradient. Lane b, gel transfer immunolocalization of monoclonal antibody binding to fragments generated by 24-h chymotrypsin digestion. Lane c, 7-h thermolysin digest. Coomassie blue stained SDS–polyacrylamide gel, 2–15% gradient. Lane d, 24-h thermolysin digest. Gel as in lane c. Lane e, gel transfer immunolocalization of monoclonal antibody binding to fragments generated by 7-h thermolysin digestion. Lane f, gel transfer immunolocalization of monoclonal antibody binding to fragments generated by 24-h thermolysin digestion.

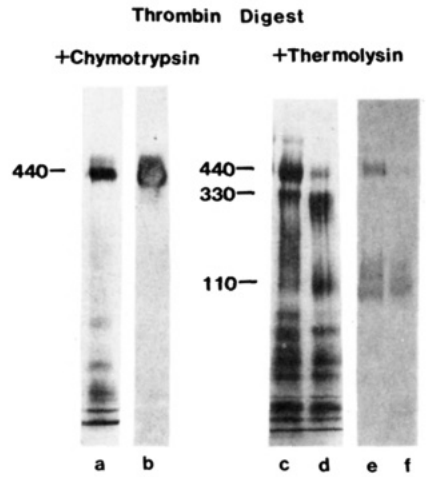

FIGURE 4: Monoclonal antibody binding to chymotrypsin and thermolysin fragments of the 600-kDa thrombin fragment of EHS laminin. Lane a, 24-h chymotrypsin digest of the thrombin fragment. Coomassie blue stained SDS–polyacrylamide gel, 2–15% gradient. Lane b, gel transfer immunolocalization of monoclonal antibody binding to fragments of the 600-kDa thrombin fragment generated by 24-h chymotrypsin digestion. Lanes c and d, 7- and 24-h thermolysin digests of the 600-kDa thrombin fragment of EHS laminin, respectively. Coomassie blue stained SDS–polyacrylamide gel, 2–15% gradient. Lanes e and f, gel transfer immunolocalization of monoclonal antibody binding to fragments of the 600-kDa thrombin fragment generated by 7 and 24 h of thermolysin digestion, respectively.

thermolysin fragments and the entire 440-kDa LMN-1 binding chymotrypsin fragment could be generated from within the 600-kDa thrombin fragment. The fragments generated by 24-h chymotrypsin digestion of the 600-kDa thrombin fragment (Figure 4, lane a) were similar to those seen with chymotrypsin digestion of the intact molecule (Figure 3, lane a). A 440-kDa LMN-1 binding chymotrypsin fragment was generated from within the 600-kDa thrombin fragment (Figure 4, lane b), similar to that generated from the intact molecule (Figure 3, lane b). Likewise, 7- and 24-h thermolysin digestion of the 600-kDa thrombin fragment (Figure 3, lanes c and d, respectively) generated digestion patterns similar to 7- and 24-h

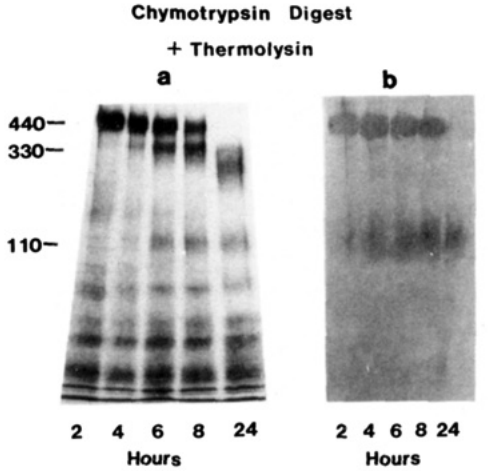

FIGURE 5: Monoclonal antibody binding to thermolysin fragments of laminin following 24-h chymotrypsin digestion. (a) Coomassie blue stained SDS–polyacrylamide gel, 2–15% gradient. Hours marked below lanes are the duration of the thermolysin digestion after the 24 h of chymotrypsin digestion. The new fragments generated by thermolysin are indicated at 110 and 330 kDa. (b) Gel transfer immunolocalization using monoclonal antibody. Only the lower of the two new bands (110 kDa), along with the original 440-kDa fragment, binds monoclonal antibody.

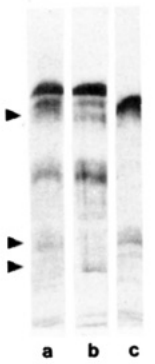

FIGURE 6: Reduced peptide map of the 440-, 330-, and 110-kDa laminin fragments generated by 7-h thermolysin digestion. Bands were cut from a nonreducing SDS–polyacrylamide gel, treated with dithiothreitol, and subjected to electrophoresis under reducing conditions. Lane a, 440-kDa thermolysin fragment; lane b, 330-kDa thermolysin fragment; lane c, 110-kDa thermolysin fragment. Arrows indicate the difference between the 440-kDa fragment (lane a) and the 330-kDa fragment (lane b).

thermolysin digestion of the intact molecule (Figure 3, lanes c and d). Both the 440- and 110-kDa antibody binding thermolysin fragments were generated from within the 600-kDa thrombin fragment (Figure 4, lanes e and f).

The thermolysin digests of laminin appeared to indicate that the 440-kDa LMN-1 binding fragment was being degraded to form the 110-kDa LMN-1 binding fragment and the 330-kDa fragment. Two approaches were used to determine whether the 110-kDa fragment came from within the 440-kDa fragment or was generated from a different region of the molecule. First, thermolysin was used to degrade the 440-kDa chymotrypsin fragment. The 440-kDa chymotrypsin fragment and the 440-kDa thermolysin fragment are thought to be similar, as Ott et al. (1982) have reported that a number of enzymes (trypsin, chymotrypsin, elastase, subtilisin, and *Staphylococcus aureus* protease) all produce a large protease-resistant fragment of laminin. Thermolysin added to a 24-h chymotrypsin digest of laminin generated both the 110- and 330-kDa fragments over time (Figure 5a). Only the original 440-kDa fragment and the newly generated 110-kDa fragment reacted with LMN-1 antibody on immunoblots (Figure 5b).

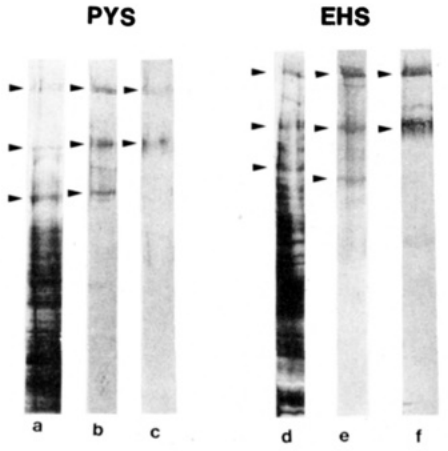

FIGURE 7: Identification of the monoclonal antibody binding subunit chain of laminin derived from PYS-2 cells and EHS cells. Lane a, Coomassie blue stained SDS–polyacrylamide gel of the PYS-2 cell extract, 2–15% gradient. Arrows indicate the intact 850-kDa molecule (top), the 400-kDa subunit chain (middle), and the 220/230-kDa subunit chains (bottom). Lane b, gel transfer immunolocalization on the PYS-2 cell extract using affinity-purified polyclonal rabbit anti-laminin antibodies. Arrows as in lane a. Lane c, gel transfer immunolocalization on the PYS-2 cell extract using monoclonal antibody. The monoclonal antibody reacts only with the intact molecule (upper arrow) and the 400-kDa subunit (lower arrow). Lane d, Coomassie blue stained SDS–polyacrylamide gel of EHS cell extract, 2–15% gradient: 850-kDa intact molecule (top arrow), 400-kDa subunit chain (middle arrow), and 200-kDa subunits (lower arrow). Lane e, gel transfer immunolocalization on the EHS cell extract using affinity-purified polyclonal rabbit anti-laminin antibodies. Arrows as in lane a. Lane f, gel transfer immunolocalization on the whole cell extract using monoclonal antibody. Antibody reacts with intact molecule (upper arrow) and 400-kDa subunit (lower arrow).

The second approach examined the disulfide-bonded structure of the thermolysin fragments by two-dimensional nonreduced/reduced peptide mapping. The second dimension reduced peptide maps of the 440-, 330-, and 110-kDa bands are shown in Figure 6. The structures of the 440- and 330-kDa fragments are nearly identical (lanes a and b, respectively). Several differences that can be seen include the following: (1) the third largest band in the 440-kDa fragment (lane a, top arrow) stains more lightly than in the 330-kDa fragment (lane b); (2) the 330-kDa fragment (lane b) has an additional lower molecular weight band (lowest arrow); and (3) there is a band in the 440-kDa fragment (lane a, middle arrow) that is not seen in the 330-kDa fragment (lane b) but is found in the 110-kDa fragment (lane c). The reduced map of the 110-kDa fragment (lane c) indicated that the fragment was predominantly one peptide of approximately 110 kDa, with lesser amounts of smaller peptides. The smaller peptides, along with heavy glycosylation, may be the cause of the diffuse appearance of the 110-kDa fragment on nonreduced gels (it appears to range from 110 to about 140 kDa). When the entire 7-h thermolysin digest was subjected to two-dimensional nonreduced/reduced peptide mapping, the 110-kDa fragment appeared to rise above the diagonal across the gel, indicating that the main peptide forming this fragment contains intrachain disulfide bonds, as well as the interchain disulfide bonds to the small peptides (gel not shown). Finding disulfide-bonded structure in this 110-kDa fragment is consistent with the LMN-1 binding data, which show that reduction of the epitope destroys LMN-1 binding activity.

Identification of the Monoclonal Antibody Binding Chain. We wanted to identify the subunit chain recognized by LMN-1. Current models of laminin fragments indicated that the site should be within one of the 200-kDa subunits (Terranova et al., 1983; Ott et al., 1982). Laminin from the PYS-2 cell line has been shown to contain two distinct 200-kDa-type chains (identified as a 220- and a 230-kDa chain) that are unique by peptide mapping (Howe & Dietzschold, 1983). Because LMN-1 binding activity was destroyed by disulfide bond reduction, laminin subunit chains had to be separated prior to final assembly. We found that sufficient amounts of precursor chains could be obtained from confluent cultures of PYS-2 cells by solubilizing cells directly into nonreducing electrophoresis sample buffer. A gel of the PYS-2 extract is shown in Figure 7, lane a. The bands consistent with the size of laminin bands (850, 400, and 220/230 kDa) are marked with arrows. [Note: Because of varying degrees of glycosylation, the 220- and 230-kDa subunits often migrate very closely together on gels and appear as one band, as in this case; also see Leivo (1983).] On immunoblots of the extracts, polyclonal rabbit antiserum stained all three subunit chains of laminin (220, 230, and 400 kDa) as well as the complete molecule (Figure 7, lane b). Unexpectedly, the monoclonal antibody identified only the 400-kDa subunit chain and the complete molecule, not any 200-kDa chains (Figure 7, lane c). As we could not be sure that the structure of PYS-2 laminin was identical with that of EHS laminin, the experiments were repeated using primary cultures of EHS cells. Figure 7, lane d, shows the complete EHS cell extract stained with Coomassie blue. Lane e is an immunoblot of the EHS extract stained with polyclonal rabbit anti-laminin. Lane f shows an immunoblot of the extract stained with monoclonal antibody. Just as with the PYS-2 extract, the polyclonal antiserum labeled the 200- and 400-kDa subunit chains of EHS laminin and the complete molecule, while monoclonal LMN-1 stained only the 400-kDa subunit and the complete molecule. There was concern that the 400-kDa band that was immunochemically stained by the monoclonal antibody might be two disulfide-bonded 200-kDa subunit chains. However, nonreduced/reduced peptide maps of the 400-kDa band indicated that this is not the case; the band remained at 400 kDa following extensive reduction with dithiothreitol (gel not shown).

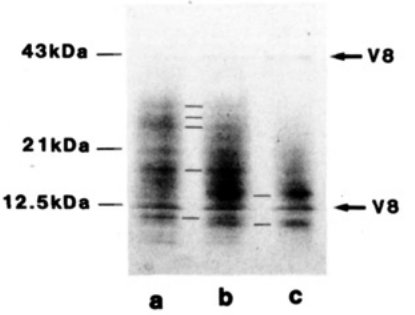

FIGURE 8: *Staphylococcus aureus* V8 protease peptide map of the 200- and 400-kDa subunits of intact laminin and the 200-kDa reduced band of the 600-kDa thrombin fragment. Lane a, peptide map of the 400-kDa subunit of laminin; lane b, peptide map of the 200-kDa band generated by reduction of the 600-kDa thrombin fragment; lane c, peptide map of the 200-kDa subunit of laminin. The lines between lanes indicate bands that the two lanes have in common. The map of the thrombin fragment (lane b) has bands in common with both the 200- and 400-kDa subunits. The arrows on the right indicate bands from the V8 protease preparation. Molecular weight standard proteins migrated as indicated on the left: ovalbumin, 43 000; soybean trypsin inhibitor, 21 000; cytochrome *c*, 12 500.

Peptide Mapping. The monoclonal antibody binding data indicated that the 600-kDa thrombin fragment contained a portion of the 400-kDa subunit of laminin. To confirm this result, and determine whether the fragment of the 400-kDa subunit was one of the three major arms of the thrombin fragment, the thrombin fragment was reduced to its constituent

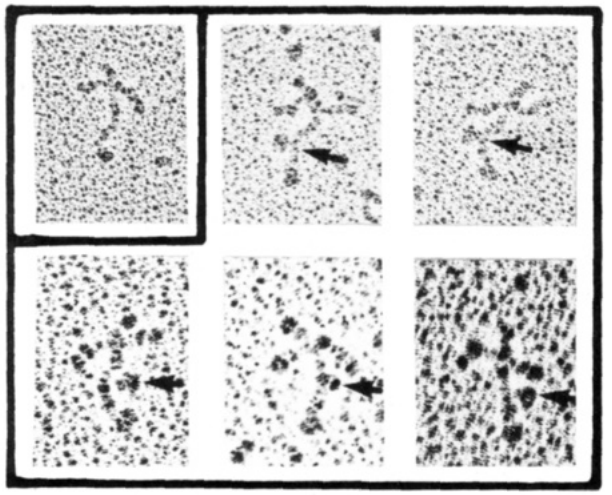

FIGURE 9: Rotary shadowing images of monoclonal antibody bound to laminin. A laminin molecule without an antibody molecule attached is shown in the upper left corner of the montage. The remaining molecules shown have an attached monoclonal antibody molecule in the middle of the long arm of laminin (arrows). Magnification 96000×.

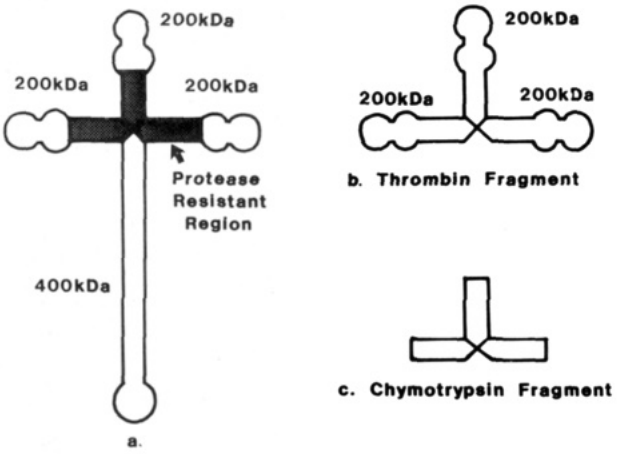

FIGURE 10: Current model of EHS laminin, based on the model of Ott et al. (1982). (a) Intact molecule consisting of three 200-kDa subunit chains and one 400-kDa subunit chain. The shaded area is the protease-resistant region. (b) Model of the 600-kDa thrombin fragment of EHS laminin, consisting of three intact 200-kDa subunit chains. (c) Model of the 440-kDa chymotrypsin fragment of EHS laminin derived from within the protease-resistant region and consisting of fragments of the three 200-kDa chains.

200-kDa chains and mapped, along with the 200- and 400-kDa subunits of intact reduced laminin, by using *Staphylococcus aureus* V8 protease (Figure 8). Lane a is the map of the 400-kDa subunit of intact laminin, lane b is the map of the 200-kDa reduced band from the 600-kDa thrombin fragment, and lane c is the map of the 200-kDa subunit of intact laminin. Lines between the lanes indicate bands that a pair of lanes have in common. The 400-kDa subunit (a) and the 200-kDa thrombin band (b) maps have five bands in common. The 200-kDa subunit (c) and the 200-kDa band from the thrombin fragment (b) have two bands in common. The bands common to all three maps marked by arrows are bands from the V8 protease preparation.

Rotary Shadowing. Rotary shadowing was used to visualize the actual physical position of the LMN-1 binding site within laminin. Molecules were examined by electron microscopy, and a record was kept of the location of antibody molecules which appeared to be bound to laminin molecules. Only laminin molecules on which all four arms could be clearly identified were considered. The LMN-1 antibody was found attached to the middle of the long arm in 110 out of 125 molecules (88%). The remaining antibody molecules were seen equally distributed among the short side arms, on the short arm opposite the long arm, and at the end of the long arm. A montage of rotary shadowing images is shown in Figure 9. In the upper left corner is a laminin molecule without monoclonal antibody bound to it. The remaining images are of laminin molecules with LMN-1 molecules attached. The monoclonal antibody is seen to bind in the middle of the long arm of laminin at a distance from the center approximately the same length as the length of the short arms.

Discussion

This study characterized a monoclonal antibody against laminin, LMN-1, and localized the antibody binding site within the laminin molecule. The data provide a basis for changes in the model of the organization of the laminin molecule. A model for the laminin molecule has been proposed by Ott et al. (1982) on the basis of rotary shadowing and gel electrophoresis studies of laminin and laminin fragments generated by proteases including elastase and subtilisin. This model is shown in Figure 10a. The model shows laminin containing three 200-kDa chains and a 400-kDa chain disulfide bonded into a cross-shaped structure. The ratio of 200- to 400-kDa chains was estimated by comparing the staining density of the two bands seen on reduced SDS–polyacrylamide gels (Engel et al., 1981). The shaded region is reported to be fairly protease resistant, resulting in the generation of a T-shaped structure following degradation with a variety of proteases (Ott et al., 1982). Terranova et al. (1983) have also done rotary shadowing on a number of laminin fragments. Thrombin was found to generate a T-shaped structure with knobs on the ends and thus was postulated to be made up of three intact 200-kDa subunit chains (Figure 10b; Rao et al., 1982b). Gel electrophoresis of thrombin-digested laminin indicated an apparent loss of the entire long arm, or putative 400-kDa subunit, leaving behind a structure presumed to consist of the 200-kDa chains (Rao et al., 1982a). The major chymotrypsin fragment was lacking the knobs and thus was thought to come from within the middle of the thrombin T structure (Figure 10c; Terranova et al., 1983). On the basis of the proposed model, and the rotary shadowing data from other laboratories, our initial hypothesis was that the LMN-1 binding site was within the 200-kDa subunit chains of laminin. The thermolysin data further indicated that if the binding were within the 200-kDa chains, not all of the 200-kDa chains were alike. If all the chains were alike, both the 330- and 110-kDa fragments would be stained by the monoclonal antibody in the immunoblot studies. However, only the 110-kDa fragment, and not the 330-kDa fragment, bound LMN-1 antibody, indicating distinct subunit chains.

The PYS-2 cell line was used to distinguish which of the 200-kDa subunits contained the LMN-1 epitope. Immunoblots of extracts of PYS-2 cells showed that LMN-1 antibody reacted with the 400-kDa subunit chain of laminin, rather than a 200-kDa subunit chain. An identical result was obtained when extracts of EHS cells were stained with monoclonal antibody. These results pointed to two possible locations for the antibody binding site within the laminin molecule. The first location, based on the assumption that the thrombin fragment was made up of the three short arms of laminin, placed the epitope in the short arm opposite the long arm of laminin. For this placement to be true, the long arm and opposite short arm of laminin would have to be comprised of only the 400-kDa subunit of laminin, as the monoclonal antibody binds to the 400-kDa subunit. A second possible lo-

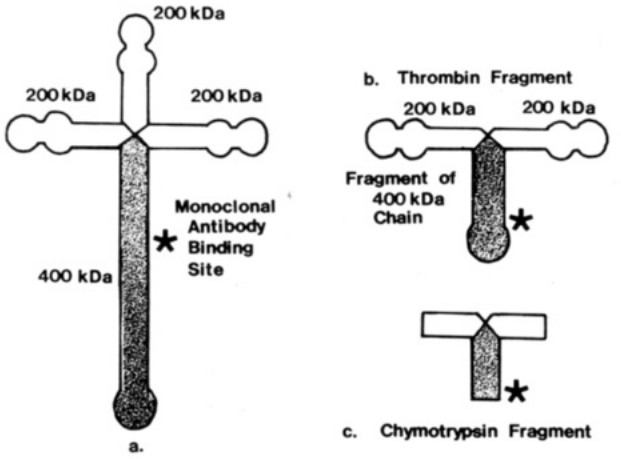

FIGURE 11: Modified model of EHS laminin based on monoclonal antibody binding to fragments of laminin. (a) Intact molecule consisting of three 200-kDa subunit chains and one 400-kDa chain. The asterisk indicates the area containing the monoclonal antibody binding site. (b) Thrombin fragment which would be generated from the molecule in (a), consisting of two 200-kDa chains and a 200-kDa fragment of the 400-kDa chain. The asterisk marks the monoclonal antibody binding region. This location is rotated 180° from the location of the thrombin fragment in the current laminin model. (c) Chymotrypsin fragment which would be generated from (a), consisting of fragments of the two 200-kDa chains and the 400-kDa chain.

cation for the LMN-1 epitope would be within the long arm of laminin, midway between the region where the four subunits join together and the far end of the long arm. This would place the thrombin fragment in a position rotated 180° from where it is located in the currently accepted laminin model (Figure 10a,b; Terranova et al., 1983). Either location of the epitope was possible, as peptide mapping confirmed that the 200-kDa band found following reduction of the 600-kDa thrombin fragment contained peptides from both the 200- and 400-kDa subunits of laminin.

Rotary shadowing of monoclonal antibody bound to laminin molecules showed that the monoclonal antibody bound to the middle of the long arm of the laminin molecule. The distance appeared to be about the same length as the short arms of laminin. Thus, we propose changes for the internal structure of laminin, as shown in Figure 11. The LMN-1 epitope is shown as an asterisk on the long arm (Figure 11a). The 600-kDa thrombin fragment is generated by partial digestion of the 400-kDa long arm and digestion of one short arm, leaving a fragment as shown in Figure 11b. The chymotrypsin fragment, which can be generated from within the thrombin fragment, is shown in Figure 11c. We have shown a globular domain on the fragment of the 400-kDa subunit in the thrombin fragment as rotary shadowing studies by several laboratories indicate that all three arms of the thrombin fragment contain globular domains (Ott et al., 1982; Rao et al., 1982b). Of some interest is that the region of the molecule which contains the antibody binding site appears to be flexible—many of the laminin molecules seen by rotary shadowing had a bend near this point. This may be contributing to the appearance of globular domains in the third arm of the thrombin fragment.

Our laminin model is based on a laminin complex containing three 200-kDa subunits and one 400-kDa subunit joined at a central point. Recent work by Barlow et al. (1984) on cDNA of the laminin B chains (200-kDa subunits) from parietal endoderm cells indicates that the chains have regions of α helix near the carboxyl terminus which may form part of the long arm of laminin, perhaps forming a double- or triple-helical structure. This would change the model of laminin from having four chains meeting at a central point to having two or possibly three of the short arms bent down and wrapped around the long arm of the molecule. The wrapping of the 200-kDa subunits around the 400-kDa subunit could confer more protease resistance to this region of the molecule by blocking access of enzymes to the 400-kDa subunit, leading to the thrombin and chymotrypsin fragments we have proposed. Another set of studies has indicated that laminin may actually only contain three subunits (Howe & Dietzschold, 1983). This group found equal synthesis of the two 200-kDa subunits and one 400-kDa subunit of laminin made by parietal yolk sac cells, indicating that laminin may have only two, not three, 200-kDa subunits. Our data would fit with a three-chain laminin structure having two short side arms consisting of 200-kDa subunits and the long arm and opposite short arm consisting of a 400-kDa subunit.

In this paper, we have described a monoclonal antibody, LMN-1, which has allowed us to immunochemically label a portion of the laminin molecule and follow it through a series of proteolytic digestions. On the basis of the data gained with this antibody, we have proposed changes in the model of the internal structure of laminin. Future immunochemical studies using this monoclonal antibody and others, along with other functional studies using affinity chromatography, will help us further define the domain structure of laminin.

ACKNOWLEDGMENTS

We thank Elaine Oberle, Richard Fuerstenberg, and Paul Marker for providing excellent technical assistance. We also thank Dr. John Sauk, Department of Oral Pathology, The University of Minnesota, for preparing the rotary shadowing specimens.

REFERENCES

Barlow, D. P., Green, N. M., Kurkinen, M., & Hogan, B. L. M. (1984) *EMBO J. 3*, 2355–2362.

Blattler, P., Garner, F., Van Slyke, K., & Bradley, A. (1972) *J. Chromatogr. 64*, 147–155.

Cleveland, D. W., Fischer, S. G., Kirschner, M. W., & Laemmli, U. K. (1977) *J. Biol. Chem. 252*, 1102–1106.

Cooper, A. R., Kurkinen, M., Taylor, A., & Hogan, B. L. M. (1981) *Eur. J. Biochem. 119*, 189–197.

Couchman, J. R., Höök, M., Rees, D. A., & Timpl, R. (1983) *J. Cell Biol. 96*, 177–183.

Del Rosso, M., Cappelletti, R., Viti, M., Vannucchi, S., & Chiarugi, V. (1981) *Biochem. J. 199*, 699–704.

Engel, J., Odermatt, E., Engel, A., Madri, J. A., Furthmayr, H., Rohde, H., & Timpl, R. (1981) *J. Mol. Biol. 150*, 97–120.

Foidart, J.-M., Timpl, R., Furthmayr, H., & Martin, G. R. (1982) in *Immunochemistry of the Extracellular Matrix* (Furthmayr, H., Ed.) Vol. I, pp 125–134, CRC Press, Boca Raton, FL.

Howe, C. C., & Dietzschold, B. (1983) *Dev. Biol. 98*, 385–391.

Kuhn, K., Wiedemann, H., Timpl, R., Risteli, J., Dieringer, H., Voss, T., & Glanville, R. W. (1981) *FEBS Lett. 125*, 123–128.

Laemmli, U. K. (1970) *Nature (London) 227*, 680–685.

Leivo, I. (1983) *Med. Biol. 61*, 1–30.

McCarthy, J. B., & Furcht, L. T. (1984) *J. Cell Biol. 98*, 1474–1480.

McCarthy, J. B., Palm, S. L., & Furcht, L. T. (1983) *J. Cell Biol. 97*, 772–777.

Ott, U., Odermatt, E., Engel, J., Furthmayr, H., & Timpl, R. (1982) *Eur. J. Biochem. 123*, 63–72.

Ozawa, M., Sato, M., & Muramatsu, T. (1983) *J. Biochem. (Tokyo) 94*, 479–485.
Palm, S. L., & Furcht, L. T. (1983) *J. Cell Biol. 96*, 1218–1226.
Rao, C. N., Margulies, I. M. K., Goldfarb, R. H., Madri, J. A., Woodley, D. T., & Liotta, L. A. (1982a) *Arch. Biochem. Biophys. 219*, 65–70.
Rao, C. N., Margulies, I. M. K., Tralka, T. S., Terranova, V. P., Madri, J. A., & Liotta, L. A. (1982b) *J. Biol. Chem. 257*, 9740–9744.
Rohde, H., Wick, G., & Timpl, R. (1979) *Eur. J. Biochem. 102*, 195–201.
Sakashita, S., Engvall, E., & Ruoslahti, E. (1980) *FEBS Lett. 116*, 243–246.
Sauk, J. J., Krumweide, M., Cocking-Johnson, D., & White, J. G. (1984) *J. Cell Biol. 99*, 1590–1597.
Smith, D. E., & Furcht, L. T. (1982) *J. Biol. Chem. 257*, 6518–6523.
Terranova, V. P., Rohrbach, D. H., & Martin, G. R. (1980) *Cell (Cambridge, Mass.) 22*, 719–726.
Terranova, V. P., Rao, C. N., Kalebic, T., Margulies, I. M., & Liotta, L. A. (1983) *Proc. Natl. Acad. Sci. U.S.A. 80*, 444–448.
Timpl, R., Rohde, H., Robey, P. G., Rennard, S. I., Foidart, J.-M., & Martin, G. R. (1979) *J. Biol. Chem. 254*, 9933–9937.
Towbin, H., Staehelin, T., & Gordon, J. (1979) *Proc. Natl. Acad. Sci. U.S.A. 76*, 4350–4354.
Vlodavsky, I., & Gospodarowicz, D. (1981) *Nature (London) 289*, 304–306.

Matrix Free Ca^{2+} in Isolated Chromaffin Vesicles

Dietmar Bulenda and Manfred Gratzl*
Abteilung Klinische Morphologie der Universität Ulm, Oberer Eselsberg, 7900 Ulm, FRG
Received June 3, 1985

ABSTRACT: Isolated secretory vesicles from bovine adrenal medulla contain 80 nmol of Ca^{2+} and 25 nmol of Mg^{2+} per milligram of protein. As determined with a Ca^{2+}-selective electrode, a further accumulation of about 160 nmol of Ca^{2+}/mg of protein can be attained upon addition of the Ca^{2+} ionophore A23187. During this process protons are released from the vesicles, in exchange for Ca^{2+} ions, as indicated by the decrease of the pH in the incubation medium or the release of 9-aminoacridine previously taken up by the vesicles. Intravesicular Mg^{2+} is not released from the vesicles by A23187, as determined by atomic emission spectroscopy. In the presence of NH_4Cl, which causes the collapse of the secretory vesicle transmembrane proton gradient (ΔpH), Ca^{2+} uptake decreases. Under these conditions A23187-mediated influx of Ca^{2+} and efflux of H^+ cease at Ca^{2+} concentrations of about 4 μM. Below this concentration Ca^{2+} is even released from the vesicles. At the Ca^{2+} concentration at which no net flux of ions occurs the intravesicular matrix free Ca^{2+} equals the extravesicular free Ca^{2+}. In the absence of NH_4Cl we determined an intravesicular pH of 6.2. Under these conditions the Ca^{2+} influx ceases around 0.15 μM. From this value and the known pH across the vesicular membrane an intravesicular matrix free Ca^{2+} concentration of about 24 μM was calculated. This is within the same order of magnitude as the concentration of free Ca^{2+} in the vesicles determined in the presence of NH_4Cl. Calculation of the total Ca^{2+} present in the secretory vesicles gives an apparent intravesicular Ca^{2+} concentration of 40 mM, which is a factor of 10^4 higher than the free intravesicular concentration of Ca^{2+}. It can be concluded, therefore, that the concentration gradient of free Ca^{2+} across the secretory vesicle membrane in the intact chromaffin cells is probably small, which implies that less energy is required to accumulate and maintain Ca^{2+} within the vesicles than was previously anticipated.

The intracellular free Ca^{2+} concentration in nucleated cells is controlled by Ca^{2+} transport systems in the plasma membrane, the endoplasmic reticulum, and the mitochondria. In secretory cells the secretory vesicles also participate in the cellular Ca^{2+} metabolism. Concerning chromaffin cells, this statement is based on (i) the histochemical visualization of Ca^{2+} in subcellular structures (Ravazzola, 1976), (ii) the direct determination of Ca^{2+} in isolated secretory vesicles (Borowitz et al., 1965; Phillips et al., 1977; Krieger-Brauer & Gratzl, 1982), (iii) the observation of an increased Ca^{2+} content within these structures after stimulation of the cells (Borowitz, 1969; Serck-Hanssen & Christiansen, 1973), and (iv) the identification of carrier systems that catalyze the transport of Ca^{2+} across the vesicular membrane (Phillips, 1981; Krieger-Brauer & Gratzl, 1981, 1982, 1983).

Ca^{2+} uptake by the chromaffin and neurosecretory vesicles depends upon the presence of Na^+ within the vesicles, and it has been suggested that the energy needed to take up Ca^{2+} is provided by the Na^+ electrochemical gradient across the secretory vesicle membrane (Krieger-Brauer & Gratzl, 1982, 1983; Saermark et al., 1983a,b). High amounts of Ca^{2+} (40–100 nmol/mg of protein) have been found in isolated adrenal medullary secretory vesicles. Assuming a vesicle volume of 2 μL/mg of protein (Johnson & Scarpa, 1976), it can be calculated that the apparent intravesicular Ca^{2+} concentration may be as high as 20–50 mM. This implies that the vesicular Ca^{2+} concentration is about 10^5 times higher than the cytoplasmic free Ca^{2+} concentration in chromaffin cells (Knight & Kesteven, 1983). When comparing the magnitude of the Na^+ gradient with the magnitude of apparent Ca^{2+} gradient across the secretory vesicle membrane, one can

† This work was supported by the Deutsche Forschungsgemeinschaft Gr 681/2-2.

0006-2960/85/0424-7760$01.50/0